

## FINAL TECHNICAL REPORT

Grant: DE-FG03-84ER45085  
 Robert Sinclair  
 Stanford University

APPLICATION OF QUATERNARY PHASE DIAGRAMS  
 TO COMPOUND SEMICONDUCTOR PROCESSING

Isobaric, isothermal phase diagrams are a molar representation of condensed phases in equilibrium with each other at a fixed temperature, pressure, and composition. Since three or four elements are usually involved at a fabricated interface in a semiconductor device, knowledge of the appropriate ternary or quaternary phase diagram is important for optimizing the processing parameters and designing long term stability of devices. While the use of phase diagrams is well-established in the fields of metallurgy, ceramics and mineralogy, only recently have phase diagrams been employed to provide a framework for understanding thin film reactions on a substrate, encountered in semiconductor processing. Even though there are many examples of applications of ternary phase diagrams in the semiconductor literature (for instance, metallization of GaAs<sup>1</sup>, the use of refractory metal silicides for metallization layers in VLSI devices<sup>2,3</sup> and oxidation of III-V compounds<sup>4</sup>), the same is not true for quaternary phase diagrams. To date, the only application is oxidation of mercury cadmium telluride<sup>5</sup>. This lack of examples is not warranted, as four elements are often involved at a critical interface in compound semiconductor processing and devices. This paper reports on the progress made to remedy this situation by considering the application of quaternary phase diagrams to understanding and predicting the behavior of II-VI thin film interfaces in photovoltaic devices under annealing conditions. Examples, listed in Table I, include semiconductor/insulator/semiconductor (SIS) layered structures, II-VI/II-VI and III-V/II-VI epitaxial heterojunctions and oxidation of ternary compounds. Moreover, for the first time, solid solubility is taken into account for quaternary phase diagrams of semiconductor systems.

Inputting the free energies of formation at a particular temperature and pressure for all the phases in the quaternary system into a computer program, a systematic and straightforward method to calculate the quaternary phase diagram has been developed. The technique extends the thermodynamic principles and properties of the isobaric, isothermal ternary phase diagram, which have their basis in the Gibbs phase rule<sup>3</sup>, one-dimension higher. Since sulphides, selenides, and tellurides are well-characterized systems thermochemically<sup>6</sup>, all 21 quaternary phase diagrams for the systems in Table I have been calculated, including the presence of solid solubility in many of the systems (Table II). Only in the most complicated case of quaternary solid solutions has solid solubility not

RECEIVED  
 OCT 17 1984

1  
**MASTER**

DISTRIBUTION OF THIS DOCUMENT IS UNLIMITED

## **DISCLAIMER**

**This report was prepared as an account of work sponsored by an agency of the United States Government. Neither the United States Government nor any agency thereof, nor any of their employees, make any warranty, express or implied, or assumes any legal liability or responsibility for the accuracy, completeness, or usefulness of any information, apparatus, product, or process disclosed, or represents that its use would not infringe privately owned rights. Reference herein to any specific commercial product, process, or service by trade name, trademark, manufacturer, or otherwise does not necessarily constitute or imply its endorsement, recommendation, or favoring by the United States Government or any agency thereof. The views and opinions of authors expressed herein do not necessarily state or reflect those of the United States Government or any agency thereof.**

## **DISCLAIMER**

**Portions of this document may be illegible in electronic image products. Images are produced from the best available original document.**

been included in the phase diagram calculations yet, but will be by the end of December 1988 when this research project is finished. In the next two sections, the Ga-As-II-VI and Cd-Te-Zn-O phase diagrams are reviewed as examples of quaternary phase diagrams without and with solid solubility.

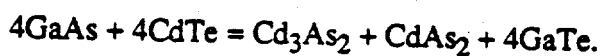
### *The Ga-As-II-VI Phase Diagram*

The equilibrium molar representation for a ternary system, the two-dimensional Gibbs equilateral triangle, becomes a three-dimensional regular tetrahedron for a quaternary system. The pure elements occupy the corners, the six binary systems the edges, and the four ternary systems the faces of the tetrahedron. Similar to ternary phase diagrams, quaternary diagrams consist of tie-lines connecting pairs of mutually stable phases, but now they pass through the tetrahedron when all four elements are involved, as well as lie on the surfaces when only three elements are needed. Tie-triangle planes, i.e. three-phase stability domains which have an irregular triangular shape bounded by tie-lines along the edges and the phases in equilibrium with each other at the corners, are formed in the interior of the tetrahedron (hence they are also given the name pseudoternary planes) and also on the faces of the tetrahedron corresponding to the ternary case. Analogous to the tie-triangle region in a ternary diagram, the building block of the quaternary diagram is the tie-tetrahedron volume which corresponds to the maximum four-phase stability domain imposed by the Gibbs phase rule. The tie-tetrahedron volume is an irregular tetrahedron bounded by tie-triangle planes on the sides, tie-lines along the edges, and the four phases in equilibrium with each other at the corners. As a result of the Gibbs phase rule, the regular tetrahedron must be completely filled by non-overlapping tie-tetrahedron volumes. Finally, the computer program determines all tie-lines in the quaternary diagram in the following manner. Constructing all possible lines between two phases and triangular planes made from these lines, the program generates a mass-balanced equation at the intersection between a possible tie-line with another line and/or a triangular plane and calculates the Gibbs free energy of reaction to establish if the tie-line is stable or not. The direction of the reaction determines the stable configuration.

This straightforward and systematic approach to quaternary phase diagrams is illustrated for the Ga-As-II-VI system (now referred to as the Ga-As-M-X system) at room temperature (298 °K) and one atmosphere pressure. Under these conditions, no solid solubility exists. Thus each phase, since it is pure and has negligible solid solubility with

all other phases, is represented by a point. The first step, presented in Figure 1, is the construction of the four ternary phase diagrams, which represent the exterior structure of the quaternary diagram, i.e. the intersection of the interior tie-triangles with the faces of the tetrahedron. All six II-VI semiconductor compounds considered here (ZnS, ZnSe, ZnTe, CdS, CdSe, and CdTe) give rise to the same form of the ternary diagrams except in one case for Se in the Ga-As-X diagram. Some of these pseudobinary tie-lines have been confirmed experimentally and published in the literature. In one case, the complete experimental diagram for the Ga-As-Zn system<sup>7</sup> is in agreement with that in Figure 1. Other examples are the ZnTe-As<sub>2</sub>Te<sub>3</sub> tie-line<sup>8</sup>, the ZnTe-Zn<sub>3</sub>As<sub>2</sub> tie-line<sup>9</sup>, and the GaAs-GaTe tie-line<sup>10</sup>. Also it has been shown that GaAs-Ga<sub>2</sub>Te<sub>3</sub> is not a true pseudobinary system, i.e. there is no tie-line between GaAs and Ga<sub>2</sub>Te<sub>3</sub><sup>10,11</sup>.

Focussing on the Ga-As-Cd-Te system only, the exterior structure of the quaternary phase diagram is shown in Figure 2. This is a true perspective of the tetrahedron. Figure 3 illustrates one calculation the computer does in determining the interior structure of the tetrahedron. Looking at Figure 3a, the Cd-As-GaTe plane is shaded, demonstrating the possibility of two interior tie-lines, GaTe-Cd<sub>3</sub>As<sub>2</sub> and GaTe-CdAs<sub>2</sub>, which would then give rise to the tie-triangle, Cd<sub>3</sub>As<sub>2</sub>-CdAs<sub>2</sub>-GaTe. However, this hypothetical tie-triangle needs to be checked against the alternate tie-line, GaAs-CdTe, according to the chemical reaction,



The free energy of reaction is positive, thus making the GaAs-CdTe tie-line the stable configuration. This result has important implications for the production of opto-electronic devices, such as CdTe-HgTe multilayers or Hg<sub>x</sub>Cd<sub>1-x</sub>Te films on a GaAs/CdTe substrate, since the original GaAs/CdTe interface will be stable as further processing is done to complete the device. The complete results for the Ga-As-Cd-Te phase diagram are depicted in Figure 4. The interior structure of the quaternary diagrams for all Ga-As-II-VI systems, summarized in Figure 5, shows all II-VI compounds in equilibrium with GaAs. Another significant outcome from these calculations is that all MGa<sub>2</sub>X<sub>4</sub> compounds are stable on GaAs, thus making GaAs a suitable substrate to grow thin films of MGa<sub>2</sub>X<sub>4</sub> compounds with their useful semiconducting and nonlinear optical properties.

Experimentally, the stability of CdTe, ZnTe and CdS on GaAs has been confirmed by carrying out x-ray diffraction of thin films annealed at 600 °C for 100 hours. Also *in situ* annealing of the GaAs/CdTe heterojunction in a high-resolution electron microscope at a nominal temperature of 500 °C for 40 minutes produced no evidence of a reaction. Crisp

near-atomic-resolution images show that while there is significant dynamic motion in the CdTe thin film itself, the interface is stable. Presently, similar work is being performed to characterize the GaAs/ZnTe and GaAs/CdS heterojunctions. Phase diagrams have also been published, which demonstrate the true pseudobinary behavior of the GaAs-CdSe and GaAs-ZnSe systems<sup>12,13</sup>.

### *The Zn-Cd-Te-O Phase Diagram*

The importance of ternary II-VI alloys for photovoltaic devices, such as tandem heterojunction solar cells, and opto-electronic devices, such as light emitting diodes, has spurred the development of alloy-growth techniques. This in turn has created a need for accurate thermochemical data and knowledge of liquid-solid phase equilibria in II-VI pseudobinary and ternary systems. Various models have been used to estimate, both theoretically and empirically, the free energy of mixing, which is the thermodynamic quantity needed to build phase diagrams for systems with solid solubility. Results from studies on determining the thermodynamic mixing parameters in II-VI solid solutions are used in this research to construct ternary and quaternary phase diagrams to predict solid state reactions. One important application is the passivation of ternary alloys by oxidizing their surfaces. Oxidation of  $Zn_xCd_{1-x}Te$  is discussed below as an example of calculating quaternary phase diagrams for systems with solid solubility.

When the  $Zn_xCd_{1-x}Te$  ternary compound is modeled as a regular solid solution with mixing parameter  $W=1.34$  kcal/mole, the known ZnTe-CdTe pseudobinary lens shape phase diagram is duplicated quite well<sup>14</sup>. Treating this continuous solid solution as nine discrete compounds across the composition range,  $x=0$  to  $x=1$ , and calculating the free energy of formation for each discrete ternary phase using the above mixing parameter value in a regular solution model, one obtains the Zn-Cd-Te room temperature ternary phase diagram in Figure 6. Along with the other ternary phase diagrams in Figure 6, the exterior structure of the Zn-Cd-Te-O quaternary diagram can be constructed as shown in Figure 7. Results from the computer analysis of the interior structure is presented in Figure 8. Confirmation of the phase diagram was obtained from x-ray diffraction of oxidized  $Zn_{.3}Cd_{.7}Te$  single crystal substrates, which produced ZnO and  $ZnTeO_3$  peaks.

### *Summary of II-VI Quaternary Phase Diagrams*

Oxidation of the other II-VI ternary alloys are summarized in Figures 9 to 11. There is no known published experimental data to test their predictions. The solid solution tie-

lines not shown here are bounded by the tie-lines between the pure phases, similar to the Zn-Cd-Te-O case. This results from the near ideality behavior in all cases.

The other oxygen containing systems, with no solid solubility however, are Cd-Te-S-O, Zn-Te-S-O and S-Se-Te-O. The reader is referred to last year's progress report for results on the Cd-Te-S-O quaternary phase diagram, which is similar to the Zn-Te-S-O phase diagram. The S-Se-Te-O phase diagram while calculated is not of technological interest and so not shown here.

Figure 12 shows the non-oxygen containing quaternary phase diagrams for II-VI systems with solid solubility. The left-hand column is for systems with ternary solid solutions only. Again the solid solution tie-lines are not shown, but are bounded by the tie-lines between the pure phases forming the endpoints of the solid solution line compounds. Solid solubility for the quaternary solid solutions in the right-hand column has not been taken into account yet. Experimental results from x-ray diffraction of annealed CdS plus ZnTe powders verify the reaction products CdTe and ZnS plus their ternary solid solutions. Experiments are currently underway to study the corresponding thin film reaction between ZnTe and CdS using *in situ* high temperature annealing in an HREM equipped with a video recorder, thus allowing direct observations of the mechanisms by which this reaction occurs at the atomic level. Other researchers have also confirmed with x-ray diffraction the reaction products CdTe, ZnS and their ternary solid solutions from annealed CdS and ZnTe powders<sup>15,16</sup> as well as from the epitaxial thin film structure<sup>17</sup>. Quasi-binary behavior, i.e. a tie-line between the two phases, has also been demonstrated for CdSe-ZnS<sup>18</sup> and ZnSe-CdTe<sup>19</sup>. The former result is in agreement with the phase diagram prediction in this report while the latter one is not. However, the predicted ZnTe-CdSe tie-line is stable only by 0.6 kcal/mole, which is within experimental error and therefore not a reliable prediction.

This report has summarized the work done on phase equilibria in II-VI quaternary systems over the last year. In general, the phase diagram depicts the geometric relationship among thermodynamic variables for phases in equilibrium with each other under an established set of conditions. Each type of thermodynamic system has a particular set of intensive variables which, when plotted against each other, best elucidate the equilibrium conditions. Isobaric, isothermal phase diagrams are used to predict solid state reactions in ternary and quaternary systems. This research has illustrated that a rigorous and methodical technique using the computer to construct quaternary phase diagrams can be successfully applied to a wide range of II-VI semiconductor systems, even for systems with solid solubility.

- 
- <sup>1</sup> R. Beyers, K.B. Kim and R. Sinclair, *J. Appl. Phys.* **61**, 2195 (1987).
  - <sup>2</sup> R. Beyers, R. Sinclair and M.E. Thomas, *J. Vac. Sci. Technol.* **B2**, 781 (1984).
  - <sup>3</sup> R. Beyers, *J. Appl. Phys.* **56**, 147 (1984).
  - <sup>4</sup> G.P. Schwartz, *Thin Solid Films* **103**, 3 (1983).
  - <sup>5</sup> D.R. Rhiger and R.E. Kvaas, *J. Vac. Sci. Technol.* **A1**, 1712 (1983).
  - <sup>6</sup> I. Barin, O. Knacke and O. Kubaschewski, *Thermochemical Properties of Inorganic Substances*, Springer-Berlin, 1977.
  - <sup>7</sup> W. Koster and W. Ulrich, *Z. Metallk.* **49**, 361 (1958).
  - <sup>8</sup> I.D. Olekseyuk, M.I. Golovei, I.M. Stoika and I.I. Yatskovich, *Izv. Akad. Nauk SSSR, Neorgan. Mat.* **11**, 2081 (1975).
  - <sup>9</sup> I.D. Olekseyuk, M.I. Golovei and N.A. Goryunova, *Izv. Akad. Nauk SSSR, Neorgan. Mat.* **7**, 747 (1971).
  - <sup>10</sup> M.B. Panish, *J. Electrochem. Soc.* **114**, 91 (1967).
  - <sup>11</sup> J.C. Woolley and B.A. Smith, *Proc. Phys. Soc. (London)* **72**, 867 (1958).
  - <sup>12</sup> V.M. Glazov, L.M. Pavlova and L.I. Perederii, *Izv. Akad. Nauk SSSR, Neorgan. Mat.* **19**, 193 (1983).
  - <sup>13</sup> V.M. Lakeenkov, M.G. Mil'vidskii and O.V. Pelevin, *Izv. Akad. Nauk SSSR, Neorgan. Mat.* **11**, 1311 (1975).
  - <sup>14</sup> P. Letardi, N. Motta and A. Balzarotti, *J. Phys. C: Solid State Phys.* **20**, 2853 (1987).
  - <sup>15</sup> V.N. Tomashik, G.S. Oleinik and I.B. Mizetskaya, *Izv. Akad. Nauk SSSR, Neorgan. Mat.* **14**, 1838 (1978).
  - <sup>16</sup> A.G. Fischer and R.J. Paff, *J. Phys. Chem. Solids* **23**, 1479 (1962).
  - <sup>17</sup> M. Aven and H.H. Woodbury, Contract AF19 (604) report AFCRL **62-141**, 27 (1962).
  - <sup>18</sup> V.N. Tomashik, G.S. Oleinik, I.B. Mizetskaya and G.N. Novitskaya, *Izv. Akad. Nauk SSSR, Neorgan. Mat.* **17**, 17 (1979).
  - <sup>19</sup> G.S. Oleinik, V.N. Tomashik, I.B. Mizetskaya, G.N. Novitskaya and V.P. Chalyi, *Izv. Akad. Nauk SSSR, Neorgan. Mat.* **13**, 1976 (1977).

**TABLE I**  
**QUATERNARY SYSTEMS OF INTEREST**

QUATERNARY SYSTEMS	APPLICATION		
	<u>HETEROJUNCTIONS</u>	<u>SIS STRUCTURES</u>	<u>OXIDATION</u>
1. Zn-Cd-O-S	ZnO/CdS; ZnS/CdO	ZnS/oxide/CdS	ZnCdS
2. Zn-Cd-O-Se	ZnO/CdSe; CdO/ZnSe	ZnSe/oxide/CdSe	ZnCdSe
3. Zn-Cd-O-Te	ZnO/CdTe; CdO/ZnTe	ZnTe/oxide/CdTe	ZnCdTe
4. Zn-Cd-S-Se	ZnSe/CdS; CdSe/ZnS	—	—
5. Zn-Cd-S-Te	ZnS/CdTe; CdS/ZnTe	—	—
6. Zn-Cd-Se-Te	ZnSe/CdTe; CdSe/ZnTe	—	—
7. Zn-O-S-Se	—	ZnS/oxide/ZnSe	ZnS <sub>2</sub> Se
8. Zn-O-S-Te	—	ZnS/oxide/ZnTe	—
9. Zn-O-Se-Te	+	ZnSe/oxide/ZnTe	ZnSeTe
10. Zn-S-Se-Te	—	—	—
11. Cd-O-S-Se	—	CdS/oxide/CdSe	CdS <sub>2</sub> Se
12. Cd-O-S-Te	—	CdS/oxide/CdTe	—
13. Cd-O-Se-Te	—	CdSe/oxide/CdTe	CdSeTe
14. Cd-S-Se-Te	—	—	—
15. O-S-Se-Te	—	—	—
16. Ga-As-Zn-S	GaAs/ZnS	—	—
17. Ga-As-Zn-Se	GaAs/ZnSe	—	—
18. Ga-As-Zn-Te	GaAs/ZnTe	—	—
19. Ga-As-Cd-S	GaAs/CdS	—	—
20. Ga-As-Cd-Se	GaAs/CdSe	—	—
21. Ga-As-Cd-Te	GaAs/CdTe	—	—

**TABLE II**  
**SOLID SOLUBILITY IN II-VI SEMICONDUCTOR BASED**  
**QUATERNARY SYSTEMS**

QUATERNARY SYSTEMS	SOLID SOLUTIONS	
_____	<u>TERNARY</u>	<u>QUATERNARY</u>
1. Zn-O-S-Te	_____	_____
2. Cd-O-S-Te	_____	_____
3. O-S-Se-Te	_____	_____
4. Ga-As-Zn-S	_____	_____
5. Ga-As-Zn-Se	_____	_____
6. Ga-As-Zn-Te	_____	_____
7. Ga-As-Cd-S	_____	_____
8. Ga-As-Cd-Se	_____	_____
9. Ga-As-Cd-Te	_____	_____
10. Zn-Cd-O-S	ZnCdS	_____
11. Zn-Cd-O-Se	ZnCdSe	_____
12. Zn-Cd-O-Te	ZnCdTe	_____
13. Zn-O-S-Se	ZnSSe	_____
14. Zn-O-Se-Te	ZnSeTe	_____
15. Cd-O-S-Se	CdSSe	_____
16. Cd-O-Se-Te	CdSeTe	_____
17. Zn-Cd-S-Te	ZnCdS, ZnCdTe	_____
18. Zn-S-Se-Te	ZnSSe, ZnSeTe	_____
19. Cd-S-Se-Te	CdSSe, CdSeTe	_____
20. Zn-Cd-S-Se	ZnCdS, ZnCdSe, ZnSSe, CdSSe	ZnCdSSe
21. Zn-Cd-Se-Te	ZnCdSe, ZnCdTe, ZnSeTe, CdSeTe	ZnCdSeTe

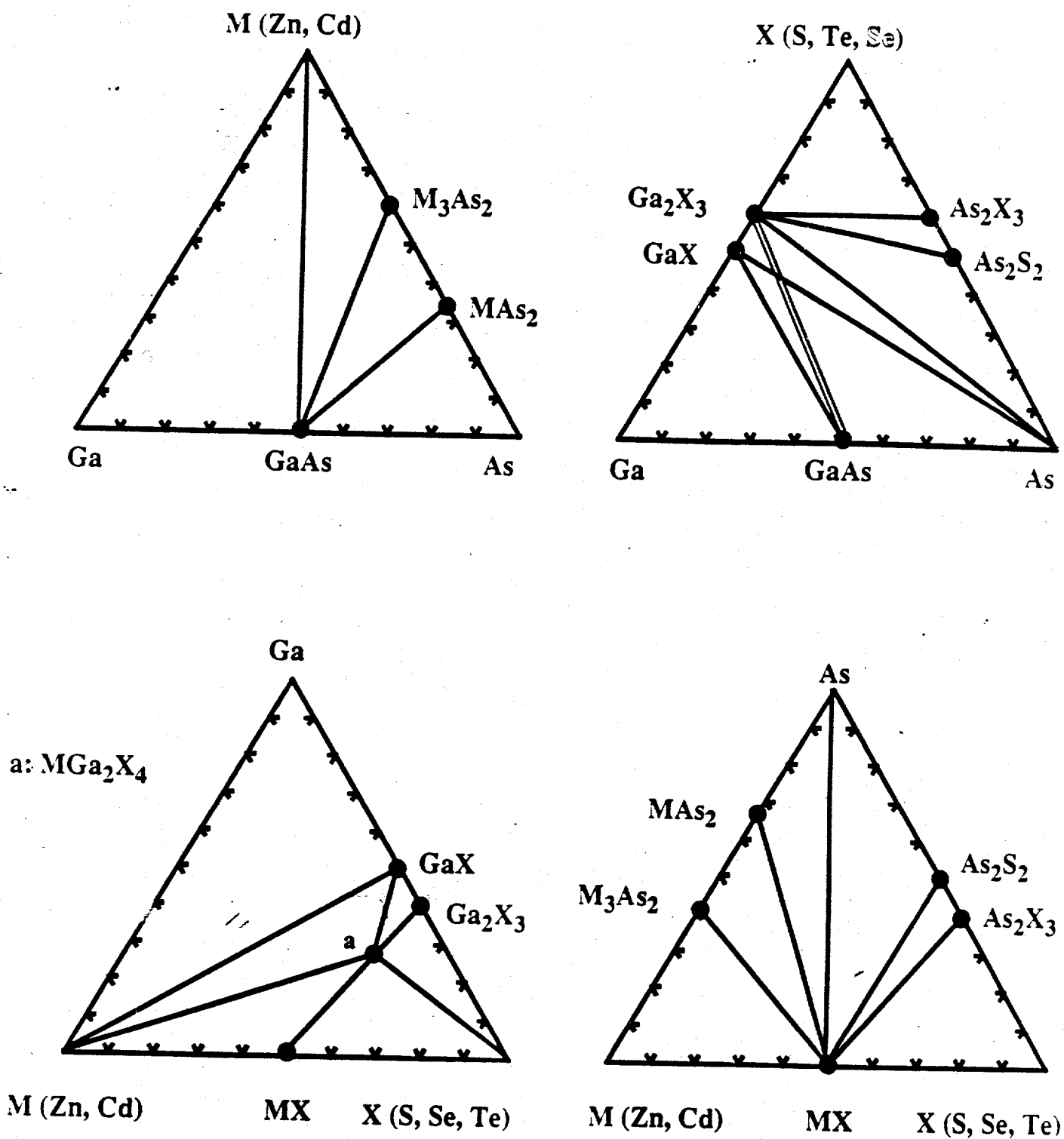


Figure 1. The four room temperature ternary phase diagrams for the Ga-As-II-VI systems. All solid black tie-lines exist for all cases except for the one intersected by the outlined tie-line for the Se case in the Ga-As-X diagram. Note that only for the sulphides, do the tie-lines emanating from  $As_2S_2$  exist.

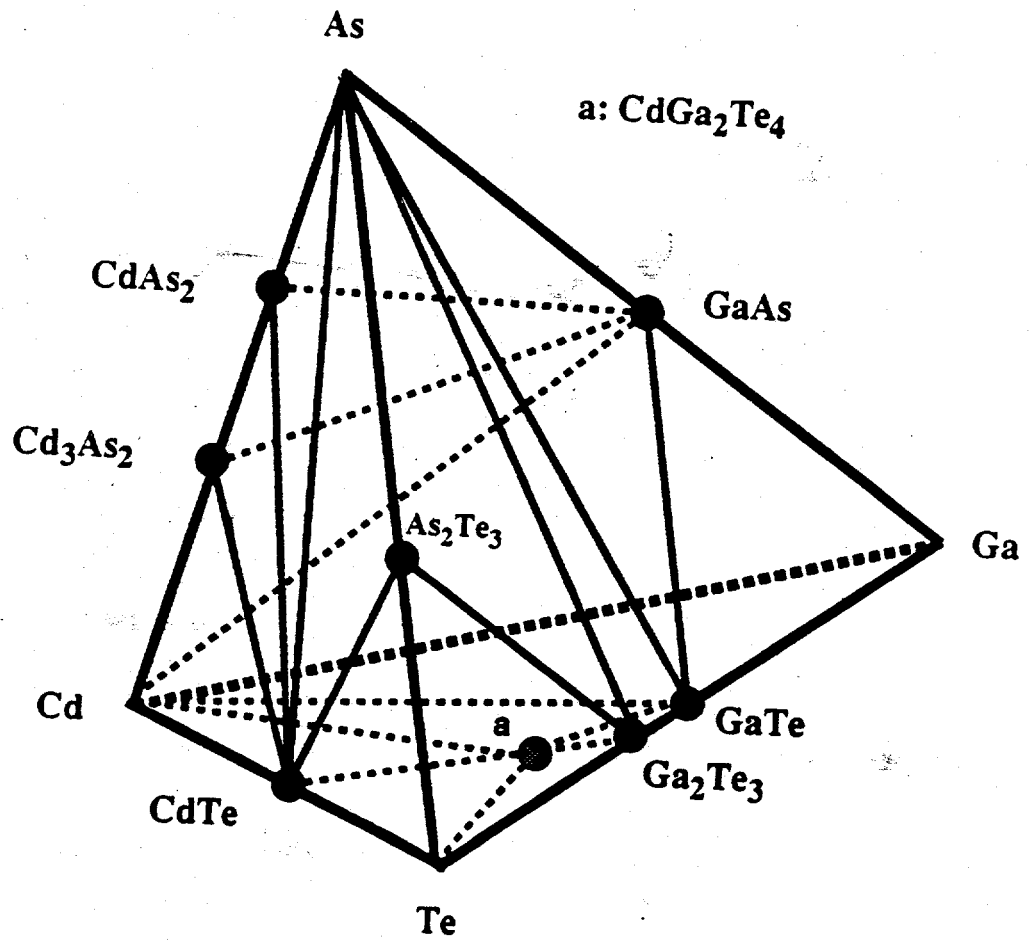
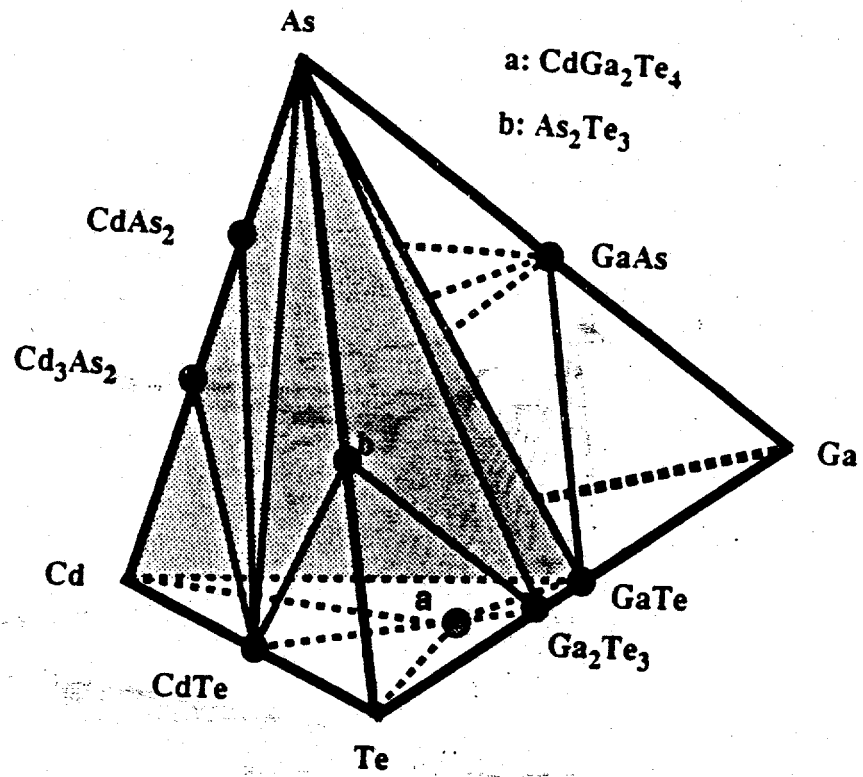


Figure 2. The exterior structure of the room temperature Ga-As-Cd-Te quaternary phase diagram.

(a)



(b)

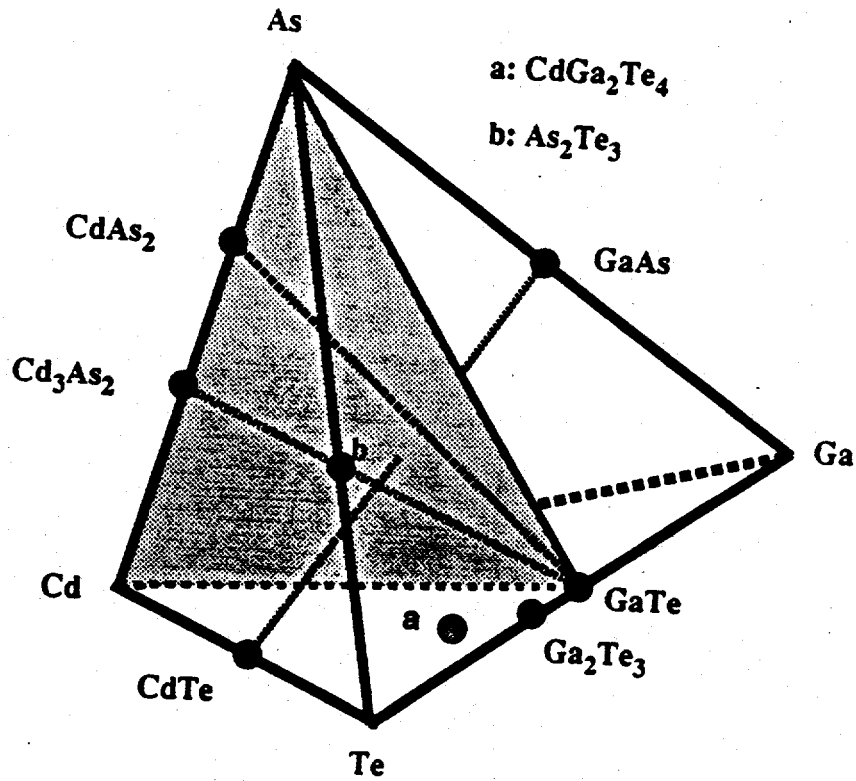


Figure 3. Construction of the interior region of the quaternary phase diagram requires comparing intersecting lines as in ternary phase diagrams as well as lines against tie-triangle planes. The Cd-As-GaTe plane is shaded (a) in order to illustrate the possible tie-triangle plane, Cd<sub>3</sub>As<sub>2</sub>-CdAs<sub>2</sub>-GaTe, which needs to be checked against the GaAs-CdTe tie-line (b). The latter case is the equilibrium configuration.

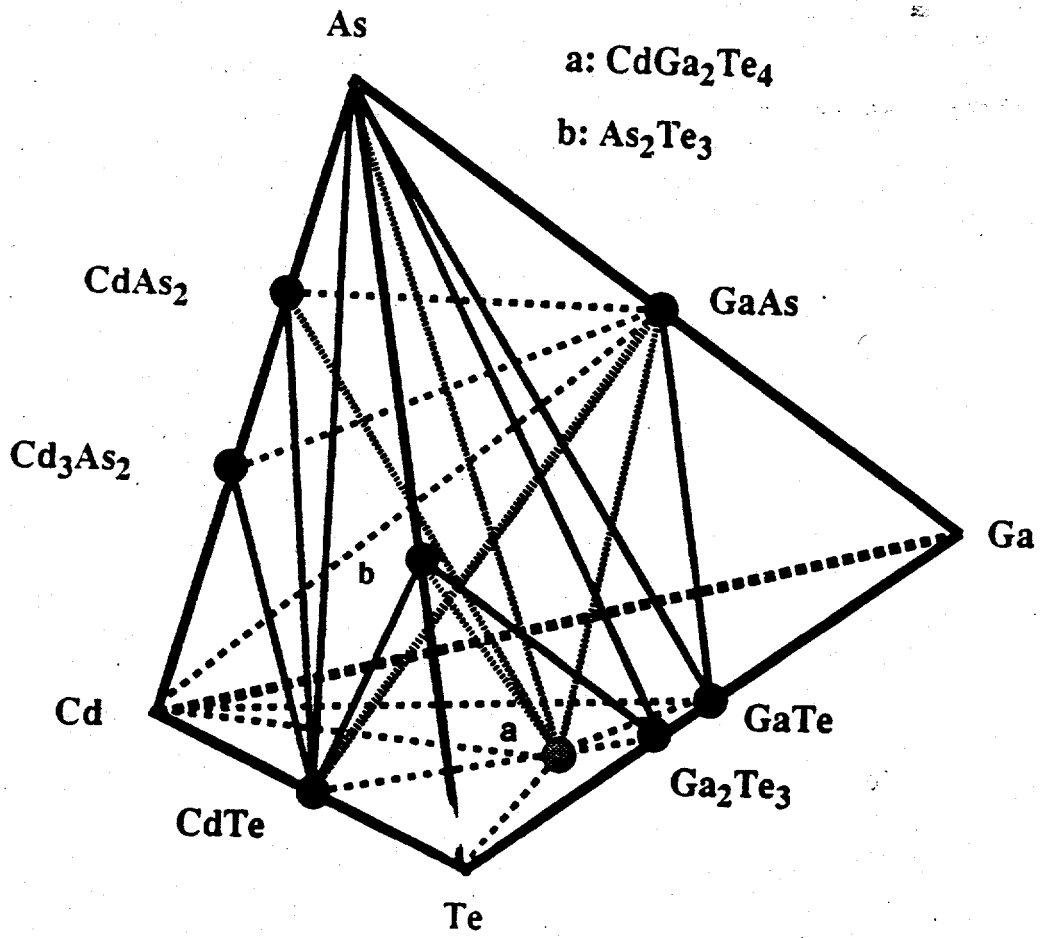


Figure 4. The complete room temperature Ga-As-Cd-Te phase diagram.

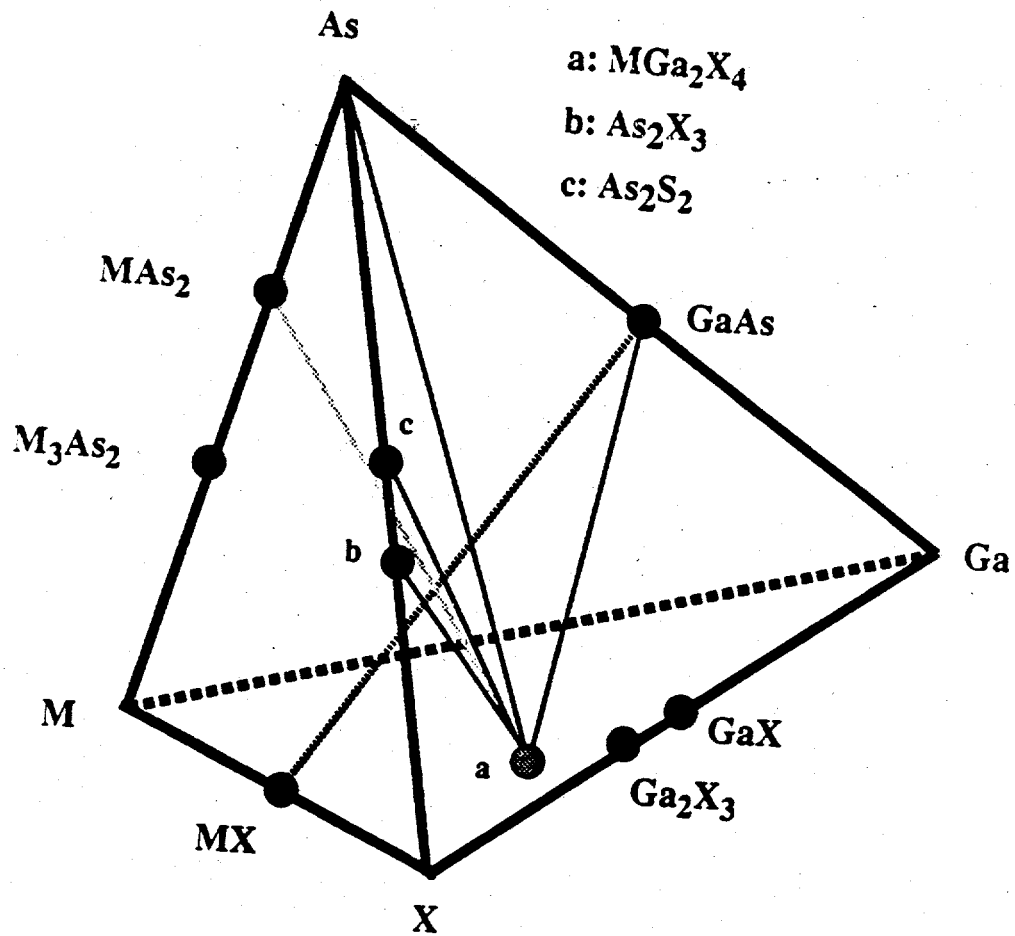


Figure 5. The room temperature interior tie-lines for the Ga-As-II-VI quaternary phase diagrams. The solid black tie-lines exist for all cases. The solid gray tie-line is true for all cases except for CdSe.

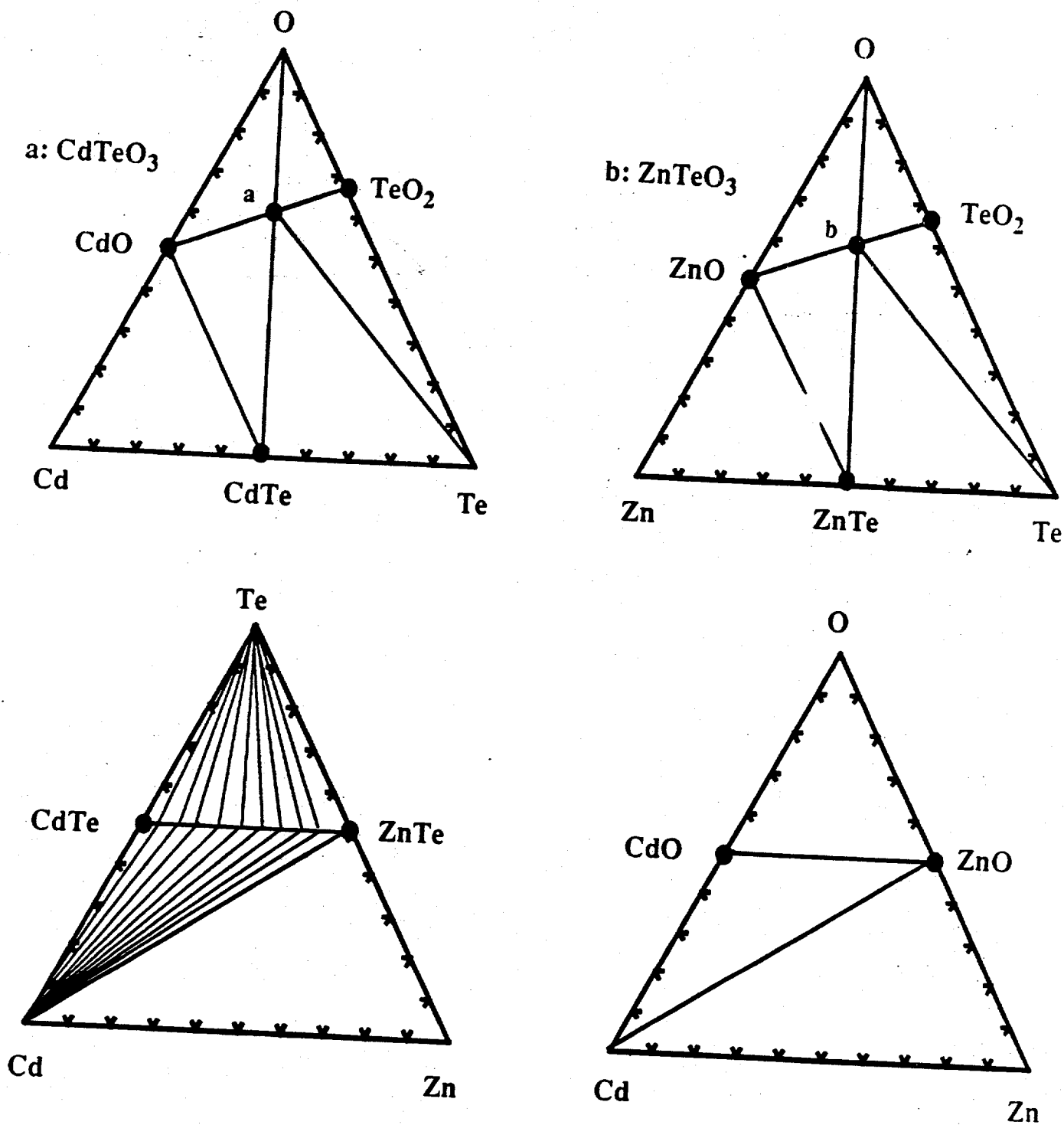


Figure 6. The four room temperature ternary phase diagrams for the Zn-Cd-Te-O system. The  $Zn_xCd_{1-x}Te$  ternary compound is treated as a regular solid solution.

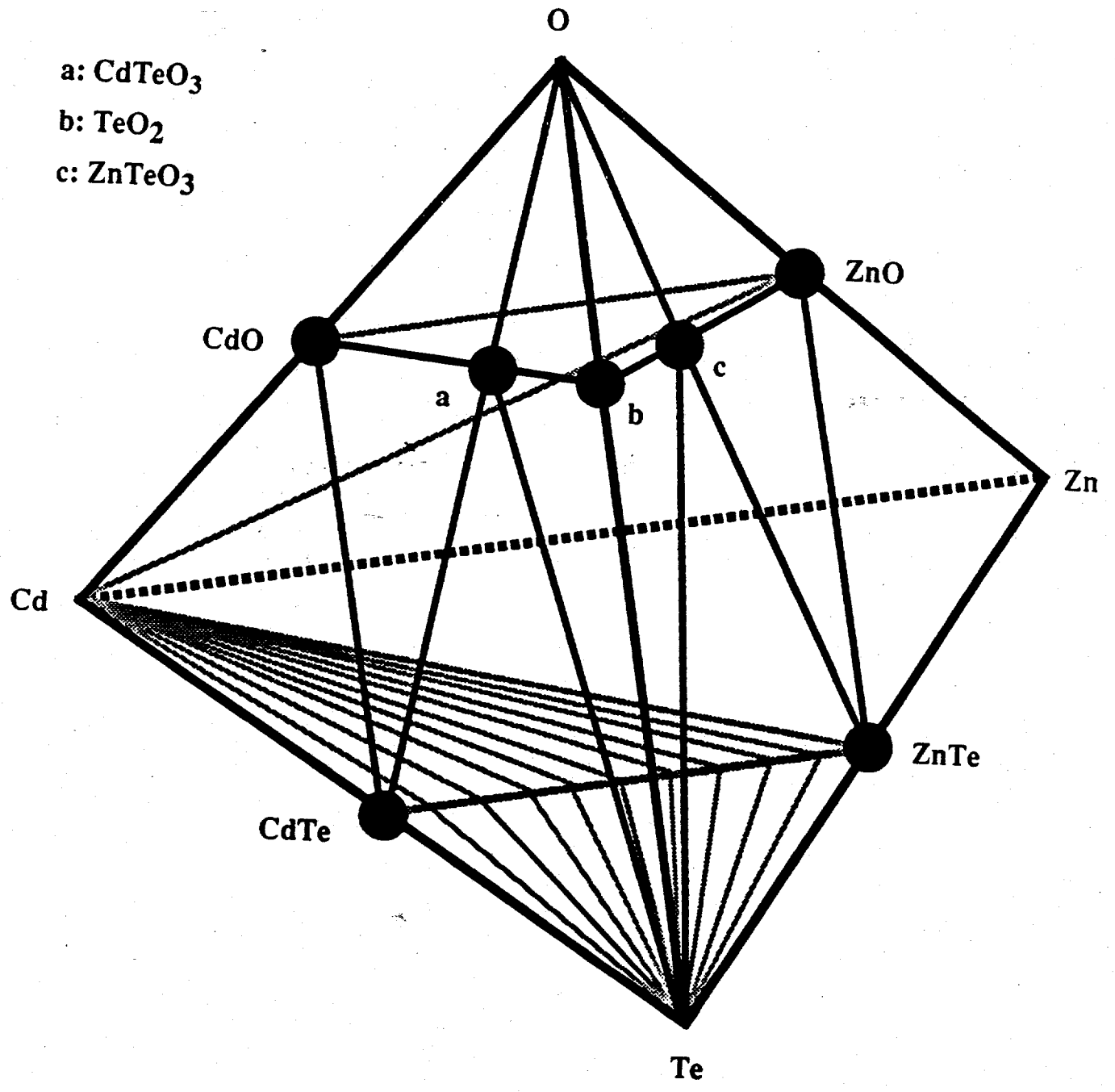
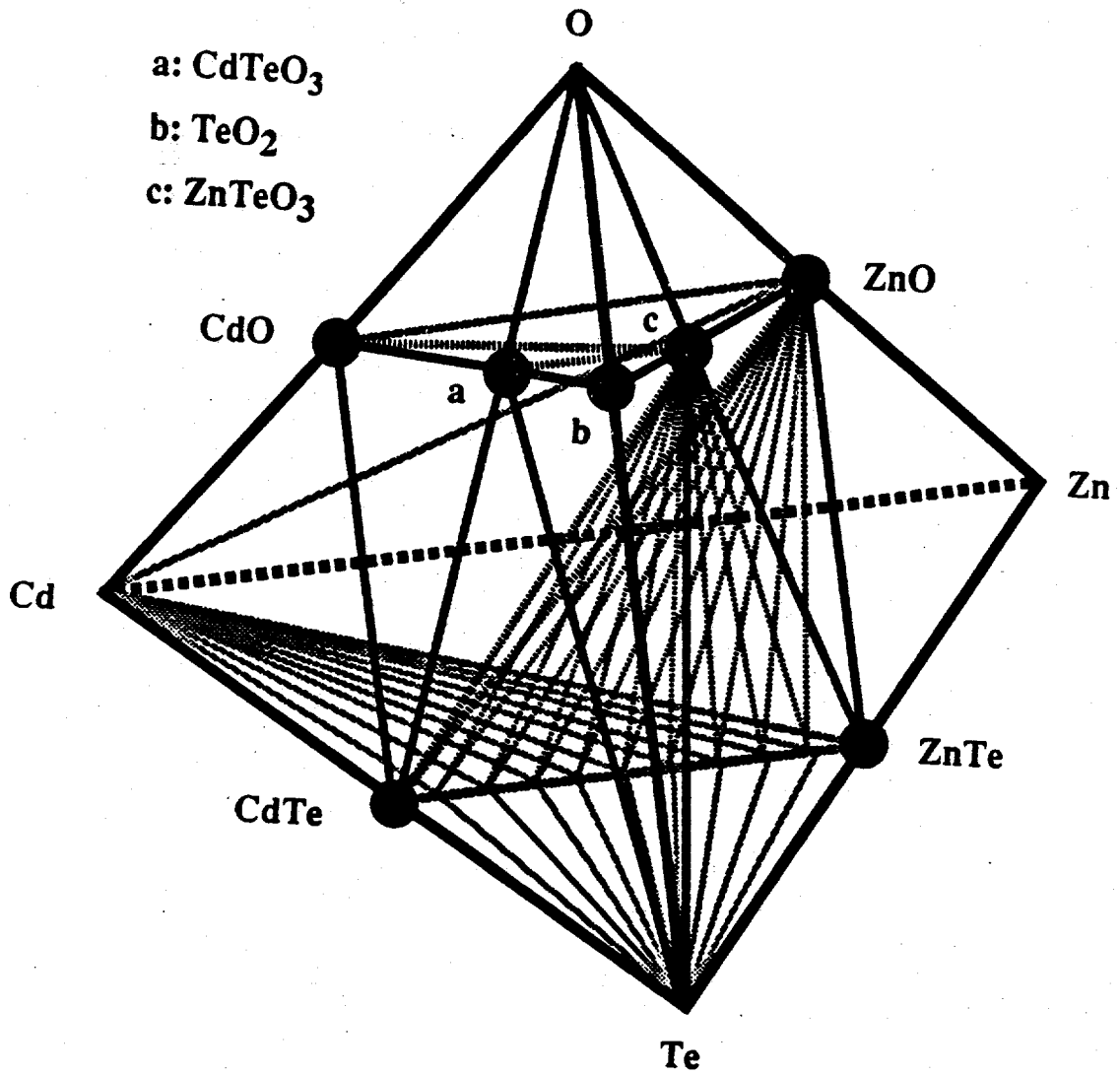


Figure 7. The exterior structure of the room temperature Zn-Cd-Te-O quaternary phase diagram. Tie-lines on the back and bottom faces are solid and shaded gray.

(a)



(b)

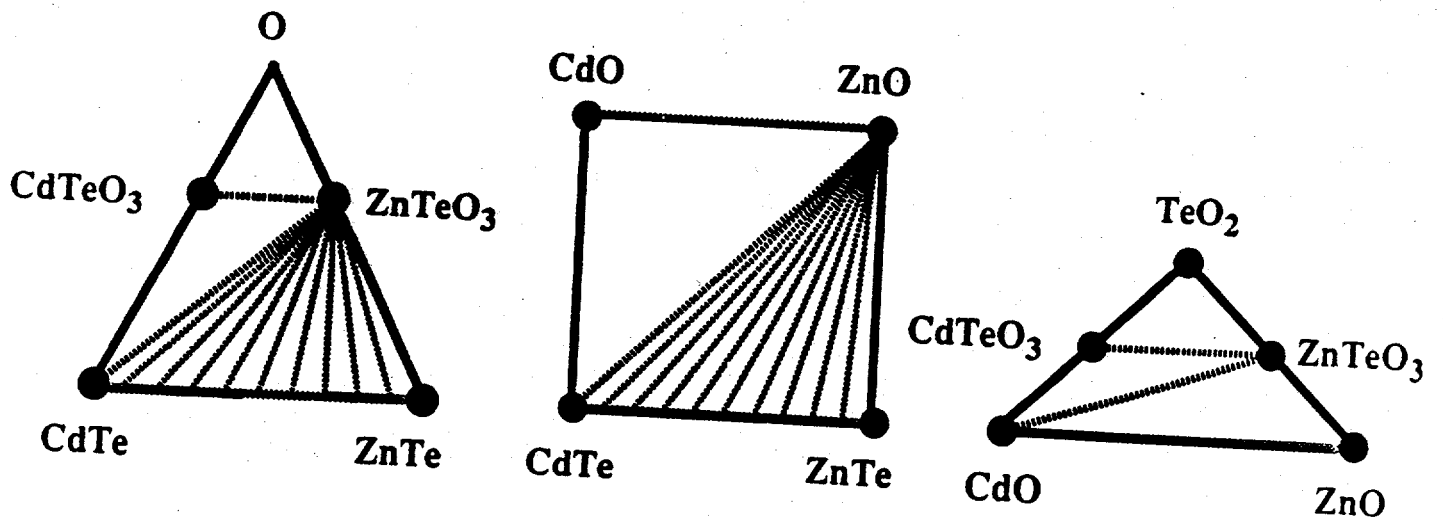
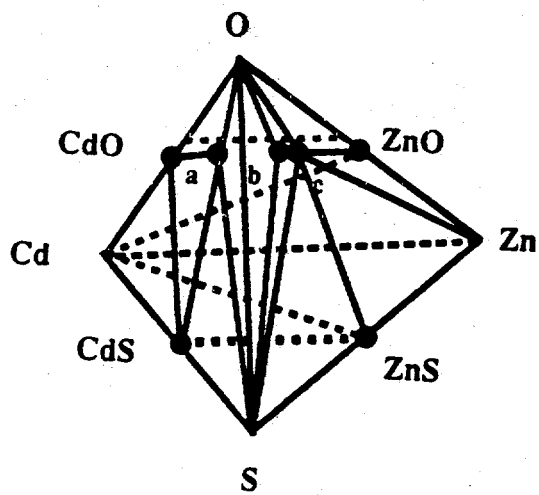
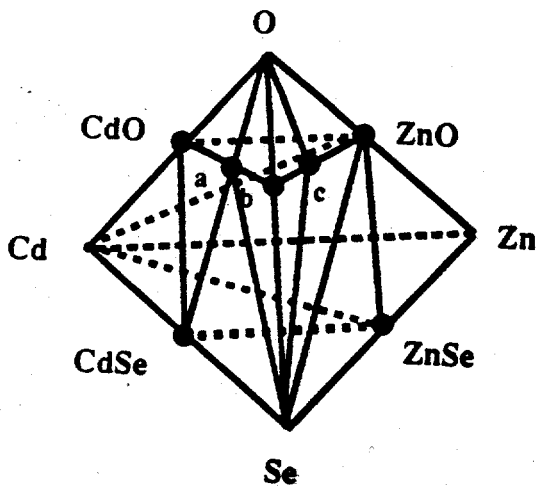
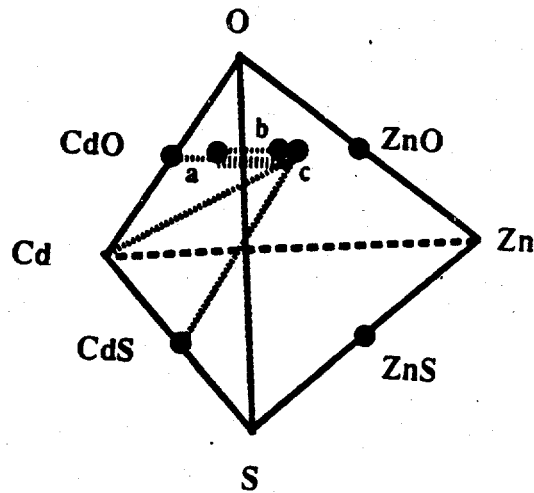


Figure 8. (a) The complete Zn-Cd-Te-O room temperature quaternary diagram.  
(b) The interior structure of the tetrahedron.



a:  $\text{CdSO}_4$   
 b:  $\text{ZnSO}_4$   
 c:  $\text{ZnO} \cdot \text{ZnSO}_4$



a:  $\text{CdSeO}_3$   
 b:  $\text{SeO}_2$   
 c:  $\text{ZnSeO}_3$

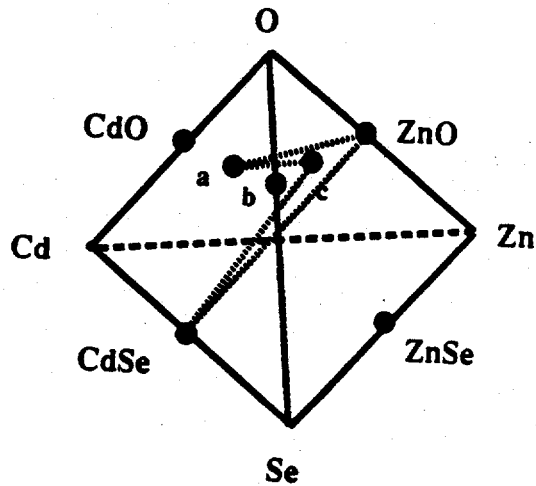


Figure 9. Quaternary phase diagrams for oxidation of cation ternary solid solutions.

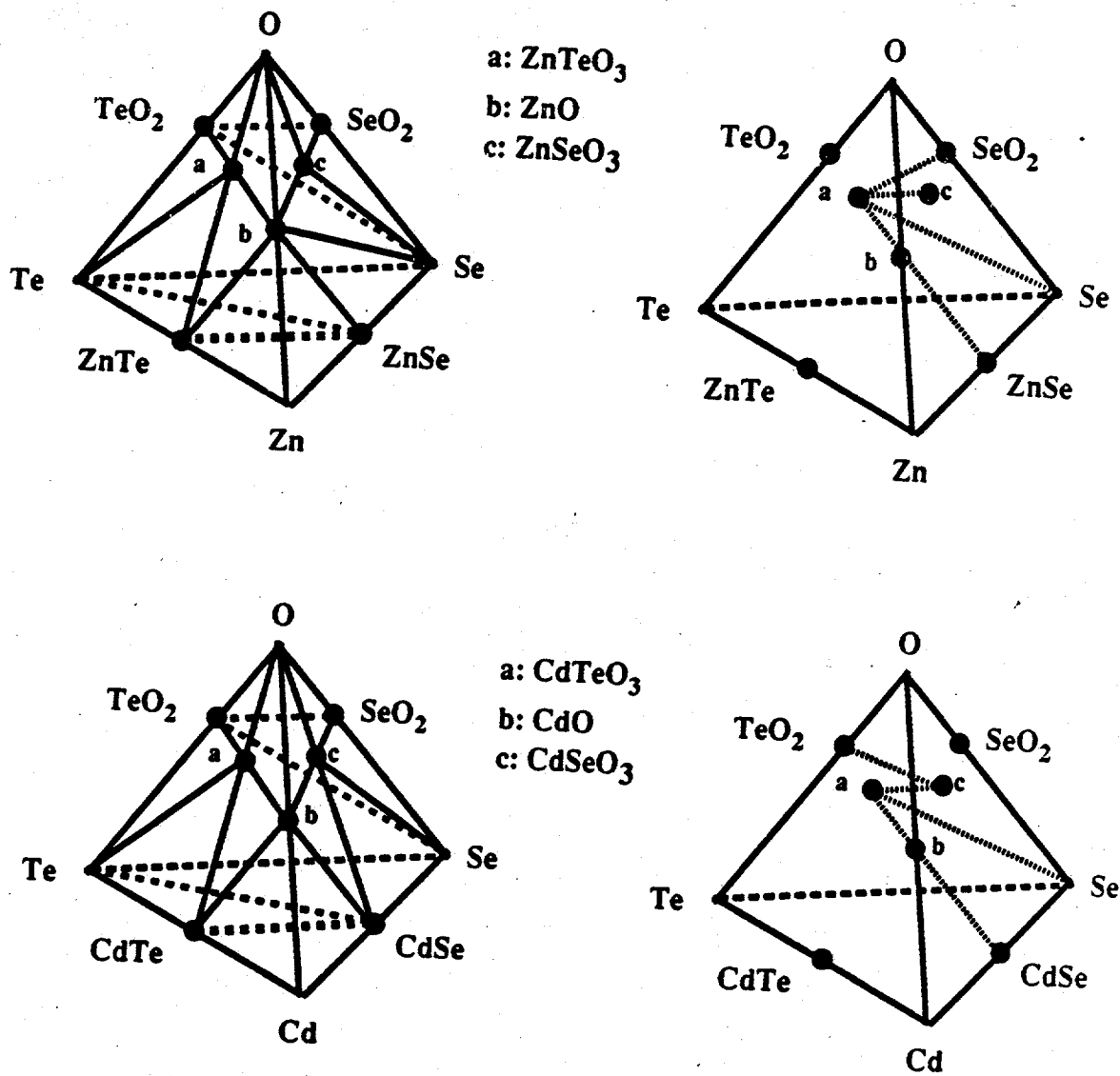
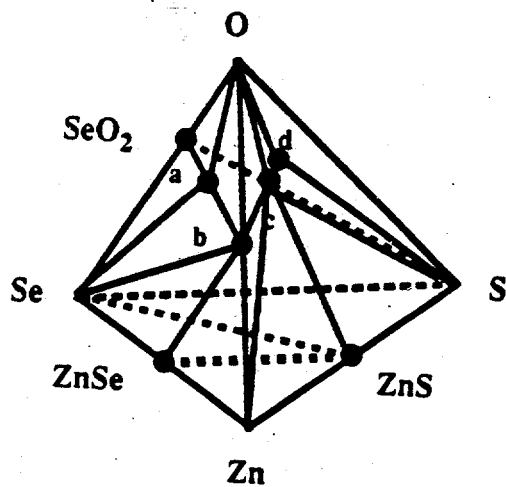
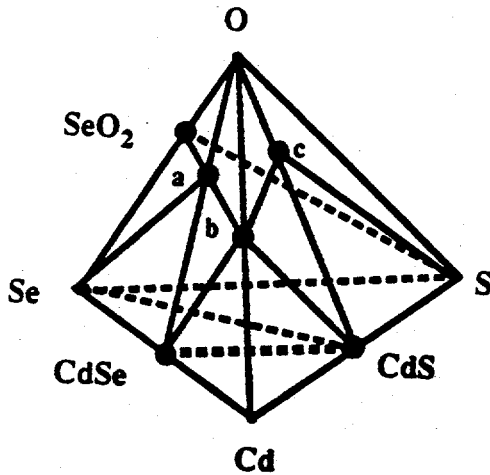
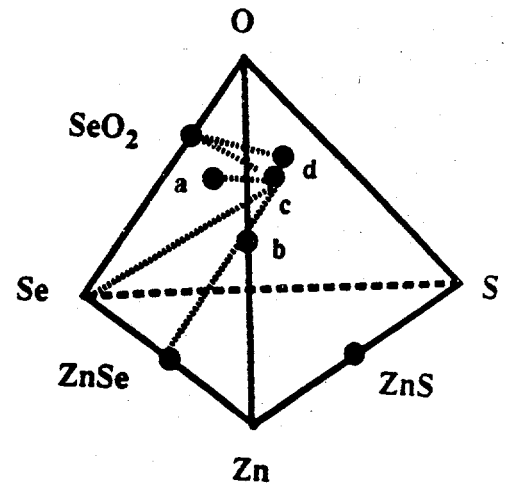


Figure 10. Quaternary phase diagrams for oxidation of anion ternary alloys based on Te/Se substitution.



- a: ZnSeO<sub>3</sub>
- b: ZnO
- c: ZnO·ZnSO<sub>4</sub>
- d: ZnSO<sub>4</sub>



- a: CdSeO<sub>3</sub>
- b: CdO
- c: CdSO<sub>4</sub>

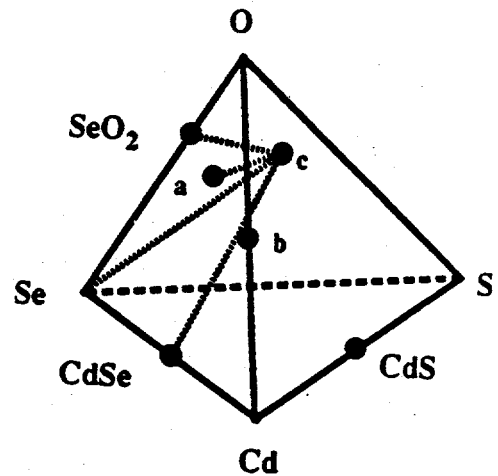


Figure 11. Quaternary phase diagrams for oxidation of anion ternary alloys based on S/Se substitution.

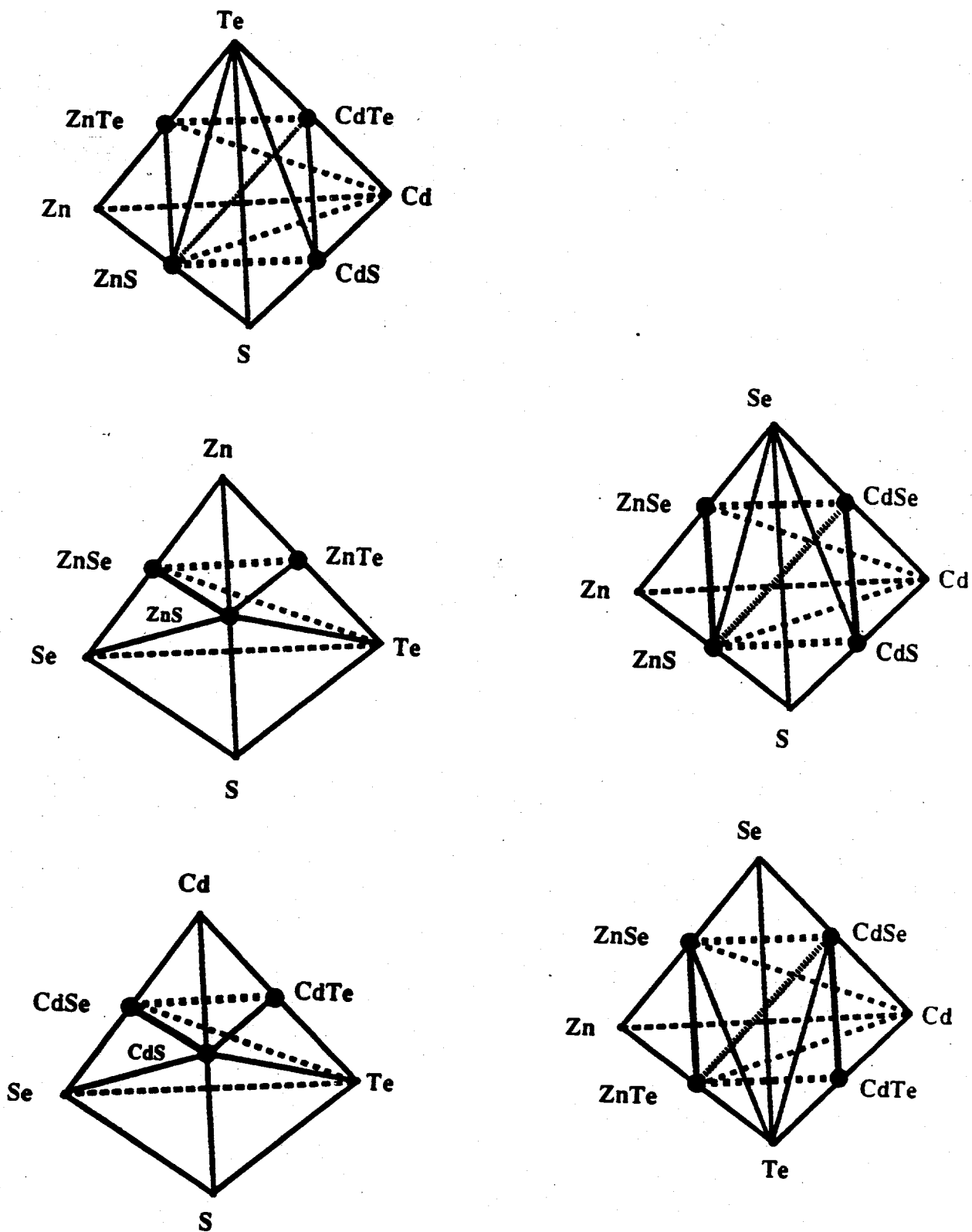


Figure 12. Non-oxygen containing room temperature quaternary phase diagrams for II-VI systems with solid solubility (heavy tie-lines). The left-hand column has ternary solid solutions only, while the right-hand side has both ternary and quaternary solid solutions. Not all tie-lines across the composition ranges are shown.